

A Hydrological Model to Evaluate Environmental Impacts due to Extensive Irrigation. Case study: Basin of the Ludueña Stream, Santa Fe, Argentina.

Erik Zimmermann, Margarita Portapila

CURIHAM, Faculty of Engineering, University of Rosario, Argentina

Wessex Institute of Technology, Southampton, United Kingdom

Abstract

A mathematical model of hydrological simulation quasi-3D is described. The model is suitable to simulate the hydrological behaviour in flat lands considering interactions between the surface zone – vadose zone (UZ) – saturated zone (SZ). The space domain is discretized in layers of surface and underground cells. In each cell, the model can quantify state variables dynamically (interception, surface storage, UZ and SZ storages) and exchange flows (evapotranspiration, infiltration, surface and groundwater flows, flow through constrictions). This aptitude of connecting surface and groundwater hydrology, enables the model to predict changes in the hydrological process due to human activities at basin scale as well as long term impacts. In this paper results of the application and calibration of the model for the Ludueña Stream System (Santa Fe, Argentina) are described. The model was run to evaluate the hydrological effects that arise out of four extensive irrigation scenarios in the Ludueña Stream basin. The simulation is done for a period of twenty years. The considered scenarios are as follows: #0 corresponds to the present situation in the basin, for which the model was calibrated. #1, #2 and #3 are three hypothetical scenarios where the soil moisture level ranges from 60% to 75% and to 90% of the field capacity, in this order. It is demonstrated that scenario #1 has not great consequences for the hydrological process and does not contribute to groundwater vulnerability. The results for scenario #2 present important consequences for the hydrological process of the real system. An increment in the recharge of the aquifer is found, modifying the groundwater table, with higher impact in low areas. The vulnerability to the contamination processes rises considerably towards the basin head. For scenario #3, the hydrological process has a very significant variation, not only for the mean and extreme hydrological values but also for the space patterns. The groundwater level is greatly increased reaching a situation of high vulnerability in terms of contamination processes. From these results, we conclude that scenarios #2 and #3 are unfeasible as far as sustainable irrigation is concerned.

1 INTRODUCTION

The use of a natural resource should be accompanied by an analysis of the effects over the involved ecosystem and its sustainability in the long run. The main objective of this work is to quantify the impact on the hydrological processes and the vulnerability of groundwater to pollution effects, when irrigation water is increased in a flatland system.

In order to do this a hydrological model capable of simulating flow and storage in the long term was developed. The model, called SHALL3, works with distributed parameters and allows a continuous operation. SHALL3 considers groundwater and surface flows, together with vertical flow –towards the aquifer and the atmosphere. The space domain is divided in interconnected cells where flow and water balances are quantified (Zimmermann and Riccardi 2000).

To ensure that the model would provide hydrological responses consistent with the studied flatland system, the conditions corresponding to the three mentioned hypothetical irrigation scenarios were generated. Therefore synthetic series of hourly storms and daily evapotranspiration were built. The analysis is made for the long term, simulating the behaviour of the system running SHALL3 over twenty years of data.

2 VERTICAL FLUXES SIMULATION IN SHALL3

Surface Hydrological Processes

The volumes intercepted by the vegetation are simulated by means of a temporary storage limited by a maximum capacity of interception, which depends on the crop type. Total precipitation is affected by the percentage of covering that depends on the cultivated area per cell, and on the crop type and its development. The surface storage is defined as the portion of rainfall that is intercepted or stored in depressions that will not reach the basin outlet. In the model the surface storage is considered as a maximum capacity to be supplied once interception has been satisfied.

Hydrological Processes in Unsaturated Zone

Moisture distribution in the vadose zone (UZ) and fluxes interchange with the atmosphere and the phreatic aquifer are calculated using Richard's equation. It was convenient to solve this equation in terms of moisture content since it allows knowing one of the variables of the hydrological balance in a direct way. The flow is considered only in the vertical direction and water extraction due to crop transpiration is reckoned.

In this work, Brooks-Corey relationships have been adopted as the retention model curve. Hysteresis between drying and wetting have not been considered.

The unsaturated porous media is discretized in cells, spanning the area from the surface to the watertable. The differential equations are solved by an explicit finite difference numerical scheme. The scheme is spatially centered and progressive in time. In the boundary of the cells flow exchanges are evaluated and in the center of the cells moisture contents are considered. Analyses of

stability and convergence have been carried out and the results of the scheme were contrasted with benchmark problems where the analytical solution is known and with other techniques and numerical schemes. Consistency was proven in all the situations, confirming the validation of the proposed scheme (Zimmermann 1998b).

Boundary conditions are imposed in the surface (upper boundary), where the infiltration is given considering precipitation and possible surplus of surface storage during a rainy period. For dry periods, if the volume intercepted and stored in surface do not cover the evapotranspiration demand, crop roots extract water of the soil. The Feddes et al. model was used to estimate the actual evapotranspiration (Candela and Varela, 1993). The model limits the rate of maximum evapotranspiration by means of a function of extraction $0 < \beta(\Psi) < 1$ where Ψ is the matrix potential. A homogeneous distribution of the roots is assumed in the soil.

For those cells in the lower boundary, which are included into the aquifer, saturation moisture is imposed as boundary condition. The group of saturated cells depends on the phreatic level, and this is calculated dynamically in the general model.

3 HORIZONTAL FLUXES SIMULATION IN SHALL3

Models that simulate horizontal fluxes, both surface and ground water, are based on cell schemes (Cunge 1975). These models simulate multidirectional flow considering the flow exchange among cells by one-dimensional flow laws.

This approach allows to divide the space domain in "layers" of homologous homogeneous sub-domains: surface and underground cells. The cells are linked by the vertical flows, as previously described. The governing equations consider in this approach are the continuity equation and the momentum equation. The latter equation, simplified in various fashions to represent the discharge between cells, complements the numerical scheme.

A spectrum of discharge laws for surface flow can be considered, such as kinematic approach, dynamic approach equation, etc. These laws allow the routing simulation for rivers, channels, flood valleys, urban streets and conduit networks. To account for local discharges from hydraulic structures laws for bridges, spillways, drains, section changes and pumping stations were developed (Riccardi 1994a, 1994b, 1997a, 1997b; Riccardi *et al*, 1995). Groundwater flow is simulated by means of Darcy's law formulation (Riccardi and Zimmermann 1999)

The continuity equation applies to each cell (Figure 1). Two hypotheses are assumed: (a) The water volume stored in a cell is directly related to its water level, and (b) the discharge between two adjacent cells at a given time is a function of the water level in the connected cells (Cunge, 1975).

The governing equations are approximated by an implicit finite difference numerical scheme. The resulting system of equations is solved using an algorithm based on the Gauss-Seidel iterative method (Riccardi and Zimmermann 1999).

Three types of boundary conditions apply: (a) water level as a function of time, (b) discharge as a function of time, and (c) water level-discharge relationship. The model requires values for the water level in all the cells at time zero.

4 IMPLEMENTATION OF SHALL3 IN THE LUDUEÑA STREAM BASIN

The Ludueña stream basin (Santa Fe, Argentina) was divided in 79 cells, 27 cells conform internal and external boundary conditions (Figure 2) and 114 matching conditions in adjacent boundaries are applied.

The unsaturated zone was divided in 70 vertical cells (depths about of 18 m.). The lower cells are submerged in the saturated zone. A spatial step of 0.25m was adopted and the temporal steps were 360 seconds. This guarantees stability and convergence conditions of the numerical scheme (Zimmermann 1998b). The vertical hydraulic conductivity for each cell was estimated using a areal weighting technique, that considers soil series, their associations, textural compositions, and saline contents (Zimmermann 2000a).

Interception storage was estimated per crop. Covering percentage and root depth were estimated considering the cultivated areas by cell, types of crops and degree of growth according to daily periods. Surface storage was detected from aerial photographs. The topography was obtained from cartography maps --scale 1:50000.

5 CALIBRATION OF THE MODEL

Although SHALL3 was conceived as a physically based model, an adjustment of parameters was necessary to reduce uncertainties or heterogeneities in the characteristics of soils (Zimmermann 2000b). Vertical and horizontal hydraulic conductivities were considered as calibration parameters. The parameter fitting was made by means of two coefficients that multiply the previously defined values. Consequently, hydraulic conductivities were fitted as lumped parameters. A good agreement between model and real system was reached (Figure 3) calculating runoff in the control section and phreatic levels in Zavalla experimental station (Figure 4).

The soil moisture estimated by the SHALL3 model in the common interfaces of cells 524 and 525 for a one meter deep, was contrasted against measured values from the Zavalla station. General tendencies in the evolution of moisture were reproduced (Figure 5). Under these conditions, the adjustment was considered satisfactory.

During the SHALL3 calibration it was checked that the biggest runoff volume was concentrated on the lower sectors of the system. The upper sectors of the hydrological system represent the recharge area. The low sectors represent the discharges of the phreatic aquifer by evapotranspiration.

6 USE OF THE MODEL FOR IRRIGATION IMPACT EVALUATION

The application of the SHALL3 model in the Ludueña Stream hydrological system was carried out under two different scenarios, *a)* Current Scenario with extensive agriculture, without massive use of irrigation and *b)* Future Scenarios with extensive agriculture and intensive irrigation. A good source of water for irrigation is the *Puelche* aquifer. This aquifer presents good water quality and high transmissivities. The *Puelche* aquifer is some 45m deep, separated from the phreatic one by a silt aquiclude. Therefore, the interaction between the *Puelche* and phreatic aquifers is can be considered as minimum. There is no quick circuit of recharge of the *Puelche* aquifer. In all cases the behaviour of the Ludueña Stream system was analysed for a twenty year period. Hence, synthetic series of hourly storms and daily evapotranspiration were specifically designed.

Synthetic series of storms

Synthetic series of storms, with similar statistical properties to the observed ones, had been previously generated (Zimmermann et al, 1996, Zimmermann 1998a). Local rainfall data was analysed through five variables: duration of the rain, time between events, average and maximum intensity of the rain and storm advance coefficient. The variables were classified into independent (first three variables) and dependent (last two variables). Probability distribution functions were fitted for the independent variables. Multiplicative relationships were proposed for dependent variables and its coefficients were previously adjusted. The statistical characteristics of the synthetic series were calculated and compared with the data series. Good agreement between calculated and measured series was obtained.

Sets of date and time of storm beginning, duration, maximum and average intensity and advance coefficient were synthetically generated. Triangular hyetographs were accepted since they presents high frequencies of occurrence (Zimmermann, 1998a). In the twenty year period of simulation 1 293 rain events were included, about 65 storms per year, totalling 952.9 mm of annual precipitation, that is widely representative of the regional statistics.

Synthetic series of evapotranspiration data

Synthetic generation of potential evapotranspiration data affected by a *tank* coefficient was carried out. In order to fit the parameters to the generating model, an observed data series (1992-1994) of tank "A" (Zavalla experimental station) was taken into account. Periodogram of observed data showed a strong component with annual frequency. A simple model was built, with a deterministic senoidal component together with a random component – a *white noise* distribution, noise with a normal distribution, null average μ and non-null variance σ .

Simulation scenarios

Current scenario. (*Scenario # 0*) The typical crops are soybean, wheat and corn. The cultivated area in the Ludueña Stream basin occupies between 85% and 90%

of the whole drainage area. Corn occupies about 10-15% of the cultivated land area while the wheat crop occupies about 15-20% and the soybean crop covers about 65-75% of cultivated land area. These percentages are dynamic, in close relation to the export market prices.

Irrigation scenarios

During the irrigation season, it should be guaranteed that the moisture state of the soil profile is kept between 60% and 90% of the field capacity, then the irrigation doses (norms) should provide the differences between the actual moisture state and the ideal one. The sequence followed by the model consisted in the following steps: a) Verify whether the date of simulation is an irrigation day. If the answer is yes, then compute the covering corresponding to this day, otherwise there is no irrigation. b) Specify the irrigation norm, as the difference (in mm) between the antecedent moisture of the soil profile and the optimum moisture, fixed as a percentage of the field capacity. c) The irrigation norm, affected by the covering coefficient, is distributed in 24 hs as a precipitation and it is operated by the infiltration subroutine. The simulations were carried out under three-irrigation hypothesis:

Scenario # 1: Optimum moisture is 60% of the field capacity during the irrigation days.

Scenario # 2: Idem with a 75% of field capacity.

Scenario # 3: idem with a 90% of field capacity.

7 RESULTS AND DISCUSSION

As previously stated the model was run for four simulation scenarios. The yearly average values, along the 20 year period, actual evapotranspiration ETR , phreatic recharge B , surface runoff Q , groundwater flow Q_G and irrigation rates IR , are shown in the Table 1.

Table 1. Yearly average values for 20 years of simulation.

	ETR (mm)	B (mm)	Q (mm)	IR (mm)	Q_G (mm)
Scenario 0	820	27	160	0	24
Scenario 1	862	52	160	102	33
Scenario 2	917	113	160	311	58
Scenario 3	947	203	172	619	72

An increment of the ETR can be observed with irrigation rate increments; there is a higher water offer to satisfy the atmospheric demand. Also, the groundwater recharge considerably increases when irrigation rates raise. The runoff does not experience variations, except for the last scenario but without establishing an important change in the magnitude of the hydrological process. It could be proven that the runoff volumes depend essentially on the rain intensity, more than on the antecedent moisture conditions Human activity in the basin has led to an impermeabilization process of the system, causing quick responses that

depend on the rainfall regime – rain intensity, magnitude and frequency (Zimmermann and Caamaño Nelli 1990, Zimmermann 1995). Table 2 shows destinations of the irrigation volumes.

Table 2. Destination (in mm and percentages) of irrigation volumes

	<i>IR</i> (mm)	<i>ETR</i> (mm)	<i>Q</i> (mm)	<i>Q_G</i> (mm)	ΔH_{ZNS} (mm)	ΔH_{ZS} (mm)
Scenario 1	102 (100%)	42 (41%)	0	9 (9%)	35 (35%)	15 (15%)
Scenario 2	311 (100%)	97 (31%)	0	34 (11%)	128 (41%)	52 (17%)
Scenario 3	619 (100%)	127 (21%)	12 (2%)	48 (8%)	304(49%)	128 (20%)

References: ΔH_{ZNS} and ΔH_{ZS} are variations of unsaturated storage and saturated storage, respectively.

Analyzing the destinations reached by the complementary irrigation would indicate that approximately between 20% to 40% of the whole volume returns to the atmosphere as *ETR*, 10% is groundwater flow and the remaining 70% to 50% would be distributed as underground storage. Runoff has little changes. The obtained results are in good agreement with previous applications of other models (Zimmermann 1999).

A distributed analysis for each simulation cell was carried out. In the natural system, the upper zone has the deeper phreatic levels (about 10 m), and the lower lands located in the center-west and northeast sectors has shallow groundwater levels (less than 3 m).

The maximum increment of phreatic levels, with regard to the scenario 0, can be found in the upper sectors of the basin, for all irrigation scenarios (Figure 6). However, the highest impacts are found in the lower sector of the catchment due to the shallow groundwater levels (Table 3).

Table 3. Average increment of phreatic levels (in m) along simulation period for representative cells of the system.

CELLS	510	516	528	530	604	608
Scenario 1	0.40	0.60	0.60	0.10	0.50	0.30
Scenario 2	1.60	2.00	1.20	0.80	1.70	1.20
Scenario 3	2.30	2.50	1.80	1.50	2.60	2.00

To analyse an average behaviour of the system in the different simulation scenarios, the typical year of the series was identified for each analysed variable. This was determined by selecting a year with the smallest deviation among the annual values and with the specified average for the whole series.

For scenario # 0, low sectors with shallow phreatic levels produce greater rates of evapotranspiration than average areal values. This space pattern was not affected in the scenarios # 1 and # 2. For scenario # 3, shallow phreatic levels appear in almost all sectors of the system, causing uniformity in the evapotranspiration rates.

The recharge for scenario # 0 shows behaviours remarkably dissimilar in upper and lower sectors, both divided by the iso-line of null recharge (Figure 7). The West sector presents the biggest phreatic depths and permeable soils, becoming the recharge area. The East sector, that includes low sectors, constitutes the discharge area.

The irrigation actions alter this scheme giving rise to isolated areas with moisture ascension and groundwater recharge according to the irrigation volumes.

Scenario #3 presents recharge processes due to the higher irrigation rates in the whole hydro-system, with the exception of the lower sector (Figure 8).

It could be observed that for scenario #0 the lower sector of the system produces the biggest runoff volumes (Figure 9).

The patterns of this space distribution are not changed with the irrigation actions. Scenario #3 causes an increase of the runoff although it is not as significant as the other hydrological processes.

The analysis mentioned so far was also carried out for dry and humid years. Significant variations in the annual totals (Table 4) but without altering the basic patterns of the system.

Table 4. Annual values for dry, typical and humid years.

Scenarios	<i>ETR (mm)</i>			<i>B (mm)</i>			<i>Q (mm)</i>		
	Dry Year.	Typ. Year	Hum. Year	Dry Year.	Typ. Year	Hum. Year	Dry Year.	Typ. Year	Hum. Year
0	692	808	904	+98	-29	-143	24	152	385
1	721	853	954	+107	-50	-164	28	152	385
2	764	918	1003	+33	-109	-206	19	155	388
3	793	946	1034	-84	-204	-276	21	181	402

Reference: *B*+ moisture ascent; *B*- recharge

The hydrological system under study, as most of the systems in the Argentinean plain, is subject to human activities that are likely to generate subsoil pollution.

The intense agricultural activity generates processes of diffuse pollution in rural areas. In this frame, extensive irrigation facilitates a quicker percolation of chemical compounds by lixiviation, mostly when the irrigation rates are not controlled. The risk of contamination is a factor that depends on the vulnerability of the aquifers and on the polluting load. The vulnerability of an aquifer represents the sensibility to be adversely affected by a polluting load (Foster and Hirata, 1988).

Vulnerability maps of phreatic aquifers are presented for scenarios #0 and #3. These maps constitute a measure of the contamination risk. For the evaluation of vulnerability indexes of the aquifer, the DRASTIC method (Vrba and Zaporozec 1994) was applied. Average depths and recharges for each aquifer cell were considered in the simulation period and for each simulation scenario.

Analysing processes of contamination due to the use of pesticides for scenario #0, it can be observed that the upper sectors of the system are found to be potentially vulnerable, with worse conditions for the north sub-sector where the

vulnerability can be considered high (Figure 10). For scenario #1 there are no important changes in the vulnerability, respect to scenario 0. For scenarios 2 and 3, the vulnerability is considerably increased. It is possible to identify two sectors in the hydrological system: an area of high vulnerability located in the upper sector and another of moderate to high vulnerability in the rest of the system (Figure 11).

8 CONCLUSIONS

It is important to highlight the versatility that presents a model based in cell schemes for modelling hydrological processes. The cells define a unit of spatial domain, which do not need to be equidistant nor to have the same physical properties. The cells can represent elements of heterogeneous characteristics linked by physical laws that correspond to the type of flow among these elements.

The hydrological model SHALL3 have allowed a detailed evaluation of the impact generated by a hypothetical extensive irrigation in the hydrological system of the Ludueña Stream. The adjustments to the runoff, phreatic levels and humidities obtained during the calibration period can be considered as satisfactory, validating the model for later simulations.

The irrigation scenario # 1 (60% of field capacity) would not bring important consequences for the hydrological processes of the real system nor would complicate the contamination process.

For the irrigation scenario # 2 (75% of field capacity), moderate increases of the annual maximum evapotranspiration and phreatic recharges are observed. This scenario would bring important consequences to the hydrological processes of the real system, mainly increasing recharges and phreatic levels with more impact in lower areas. The vulnerability to contamination processes rises considerably in the upper sectors of the system.

For the irrigation scenario # 3 (90% of field capacity), the hydrological processes suffer highly significant variations, both in the average and extreme values as well as in the space patterns, leading to an important increase in the phreatic level. Summarizing, this irrigation scenario would bring consequences of great magnitude for the hydrological processes of the whole system, as well as for the vulnerability to contamination processes. All these impacts make this irrigation hypothesis unfeasible from the environmental point of view.

Contrary to what was expected, the runoff does not reflect significant changes due to irrigation actions. This implies a sign of impermeabilization of the basin, since the runoff becomes independent of the antecedent condition and it only depends on the intensity of the rainfall.

REFERENCES

- Candela L, Varela M (1993) *La zona no saturada y la contaminación de las aguas subterráneas. Teoría, medición y modelos*; Editores Candela y Varela; CIMNE, Barcelona, España.
- Cunge J. (1975) *Two dimensional modeling of flood plains*, in: Mahmood K. and Yevjevich V., eds. *Unsteady flow in open channels*, Water Resources Publications, Fort Collins, 705-762.
- Foster S, Hirata R (1988) “*Determinación del riesgo de contaminación de aguas subterráneas*”. CEPIS – OPS – OMS. Lima. Perú.
- Riccardi, G. (1994a) *Un Modelo Matemático Hidrodinámico cuasi-bidimensional para escurrimiento cuasi-dinámicos*, XVI Congreso Latinoamericano de Hidráulica, IAHR-LAD, Santiago
- Riccardi, G. (1994b) *Aplicación de un Modelo Matemático de Celdas para escurrimientos cuasi-dinámicos en el Arroyo Saladillo*, XVI Congreso Latinoamericano de Hidráulica, IAHR-LAD, Santiago
- Riccardi G, Zimmermann E, Maurig R (1995) *Mathematical Modelling of Flood Propagation for the Delimitation of Rural, Semiurbanized and Urbanized Zones with Inundation Risk*; IAHS International Symposium on Runoff Computations for Water Proyects, St. Petersburg - Federación Rusa.
- Riccardi, G. (1997a) *The mathematical modelling of flood propagation for the delimitation of inundation risk zones*, Sustainability of Water Resources under Increasing Uncertainty (ed. D. Rosberg et al.) IAHS Publication Nro 240, ISSN 0144-7815., Wallingford, 355-364.
- Riccardi, G. (1997b) *El Mapeo de Riesgo de Inundación por medio de la Modelación Matemática Hidrodinámica*, Revista Ingeniería del Agua, Vol 4 N° 3, ISSN 1134-2196, Univ. Politécnica de Valencia, 45-56.
- Riccardi, G Y Zimmermann, E. (1999) *La Modelación Matemática Bidimensional de Escurrimiento Subterráneo mediante Esquemas de Celdas*. Hidrología Subterránea, Edit. A Tineo, Serie de Correlación Geológica N° 13, ISSN 1514-4186, Instituto Superior de Correlación Geológica-CONICET, Tucumán, 79-88.
- Vrba J, Zaporozec A (1994) “*Guidebook on Mapping Groundwater Vulnerability*”. IAH International Contribution to Hydrogeology. Vol 16. Hannover. Germany.
- Zimmermann E, Navarro R, Silber M (1996) “*Un Modelo Probabilístico para la Generación Sintética de Tormentas*”, XVII Congreso Latinoamericano de Hidráulica; IAHR; Guayaquil; Ecuador.
- Zimmermann E (1998a) *Synthetic Storm Generation in a Flatland Region (Santa Fe, Argentina)*. Journal of Environmental Hydrology. Vol. 6. N° 2. IAEH.
- Zimmermann E. (1998b) *Esquema explícito para la resolución de la ecuación de Richards*. XVII Congreso Nacional del Agua. Santa Fe. Argentina.
- Zimmermann E. (1999) *Assessment of hydrologic impacts of irrigation projects in a flatland area, Santa Fe, Argentina..* Journal of Environmental Hydrology. Vol. 7. N° 1. IAEH.

- Zimmermann E. (2000a) *Metodología para la estimación de la conductividad hidráulica equivalente en suelos no saturados heterogéneos*. Cuadernos del CURIHAM. PHI-UNESCO. Vol 6, No. 1. pp 1-12. ISSN 1514-2906. UNR Editora.
- Zimmermann E. (2000b) *Aplicación y calibración del modelo SHALL3 en el sistema hidrológico del A° Ludueña, Santa Fe Argentina*. XIX Congreso Latinoamericano de Hidráulica. Córdoba. Argentina Vol II. pp 713-722. IAHR. ISBN 950-33-0267-6.
- Zimmermann E, Riccardi G. (2000) *Modelo de simulación hidrológica superficial y subterránea para áreas de llanura*. XIX Congreso Latinoamericano de Hidráulica. Córdoba. Argentina Vol II. pp 169-178. IAHR. ISBN 950-33-0267-6.

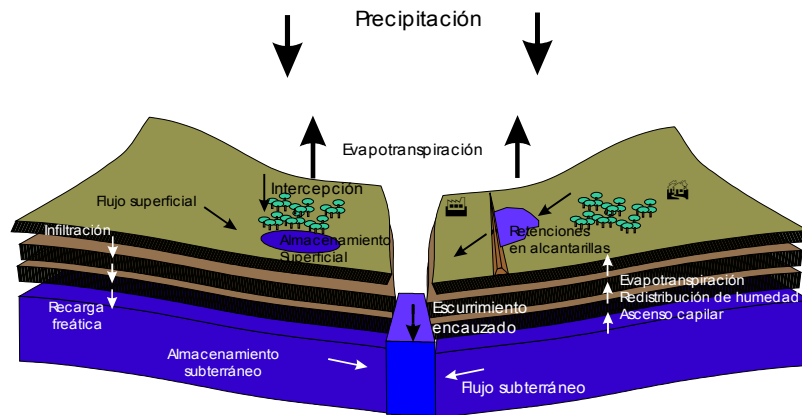


Figure 1 Scheme of assemblage between surface, unsaturated and groundwater cells

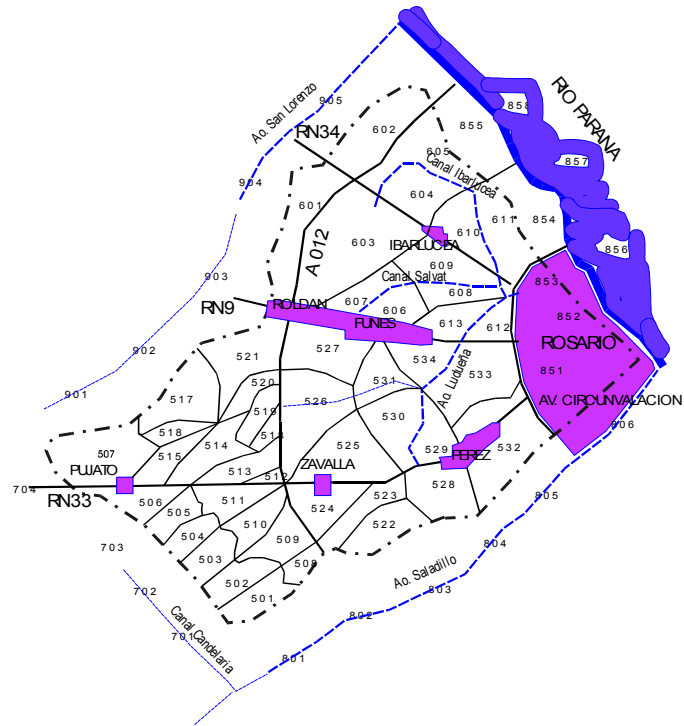


Figure 2 Ludueña system: ubication and spatial division

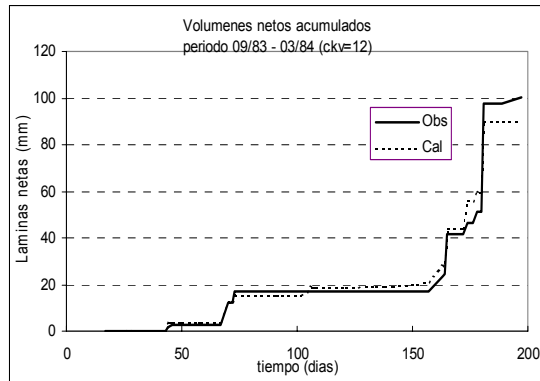


Figure 3 Observed and calculated runoff. Determination coefficient between both series: $r^2 = 0.9747$

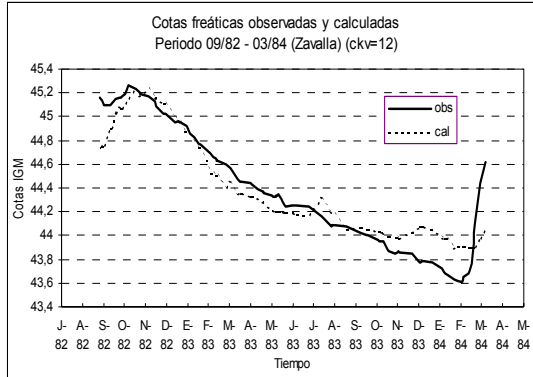


Figure 4 Observed and calculated phreatic levels. Determination coefficient between both series: $r^2 = 0.8917$

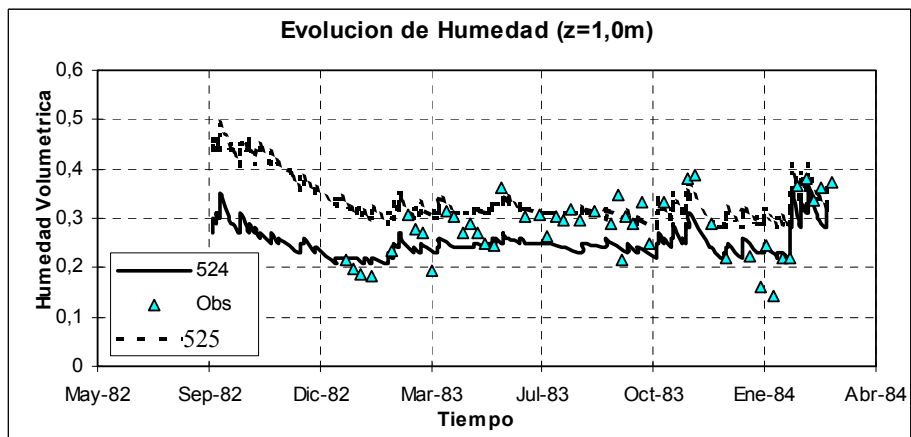


Figure 5 Moisture contents at depth 1m.

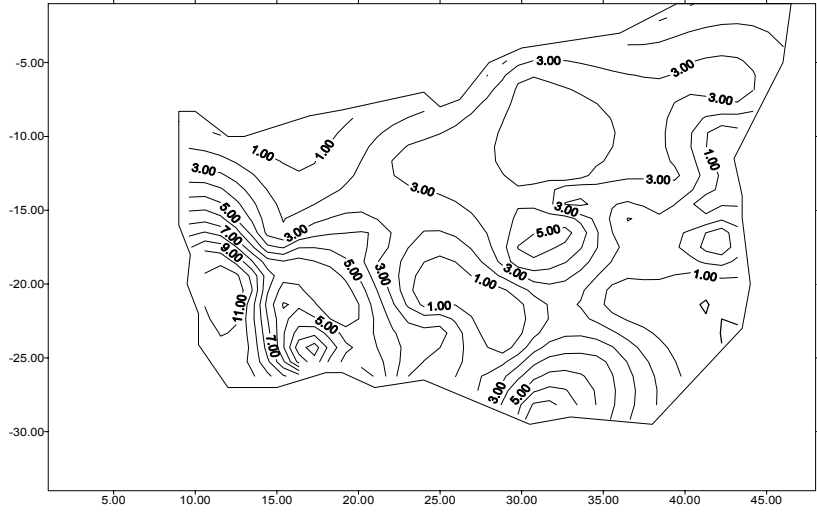


Figure 6 Increase of phreatic levels. Scenario # 3

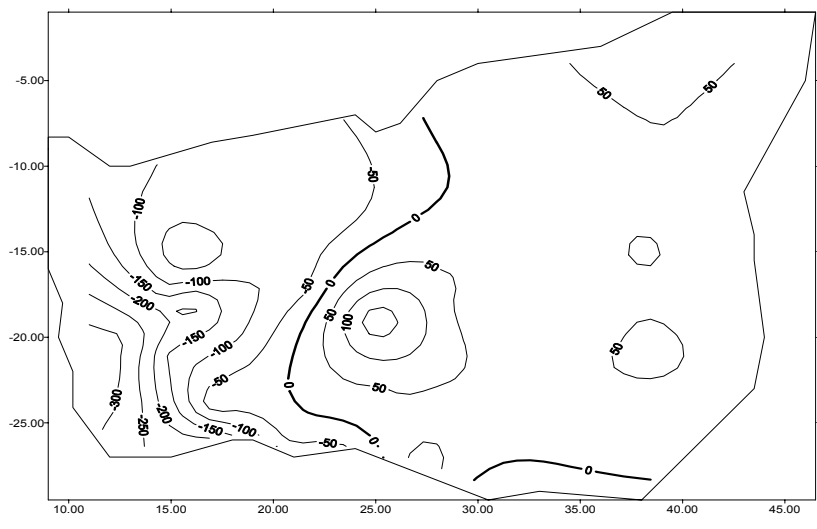


Figure 7 Recharge isolines. Scenario # 0

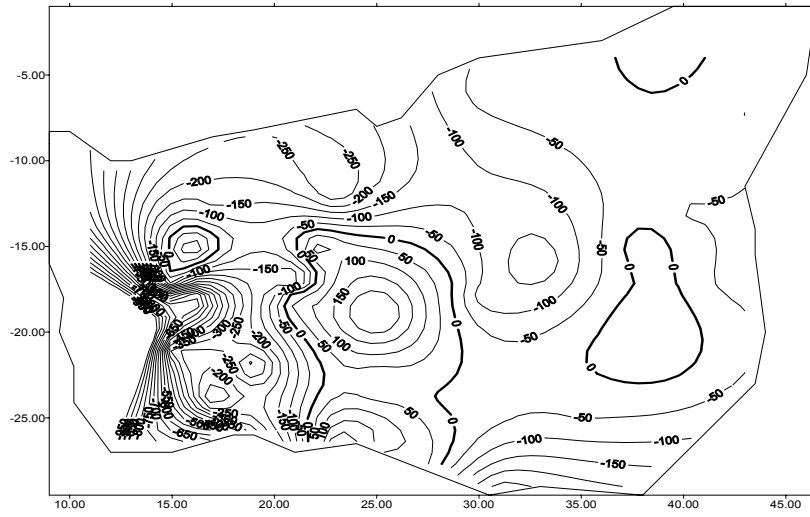


Figure 8 Recharge isolines. Scenario # 3

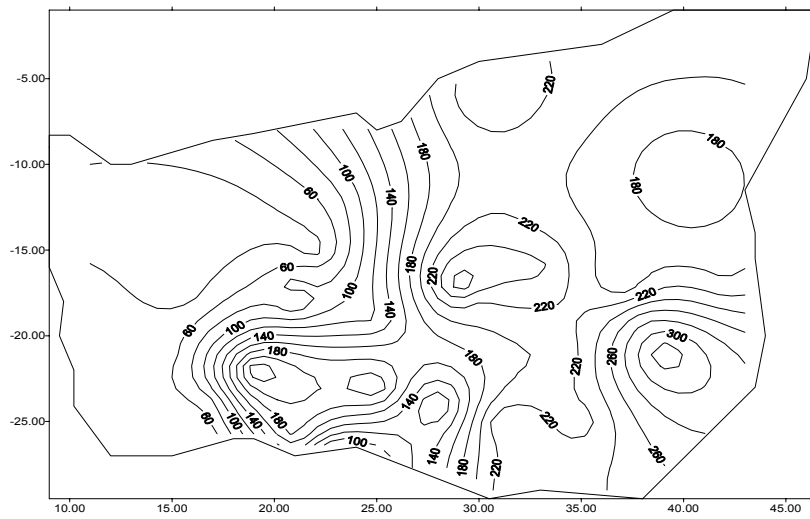


Figure 9 Runoff isolines. Scenario # 0

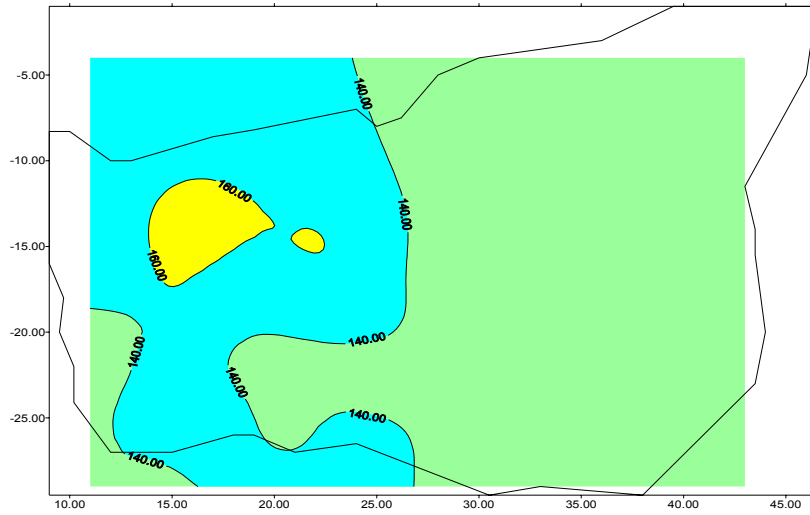


Figure 10 Vulnerability of phreatic aquifer. Scenario # 0

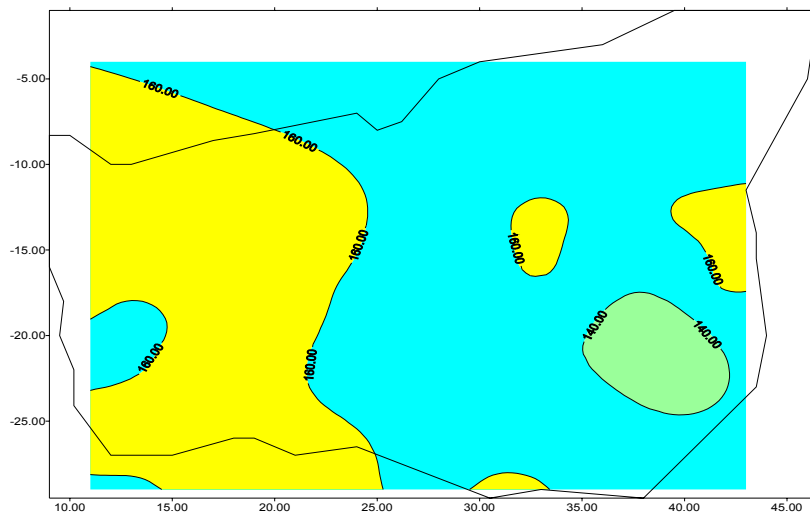


Figure 11 Vulnerability of phreatic aquifer. Scenario #